BEAM-SIZE MEASUREMENT SYSTEM AT THE SAGA-LS STORAGE RING

Y. Takabayashi#, T. Kaneyasu, Y. Iwasaki, and S. Koda
SAGA Light Source, 8-7 Yayoigaoka, Tosu, Saga 841-0005, Japan

Abstract

A beam-size measurement system has been developed at the SAGA Light Source (SAGA-LS) storage ring. The developed system consists of a beamline for visible light, a synchrotron radiation (SR) interferometer, and a data acquisition system. A client-server system using the ActiveX channel access (CA) protocol was also developed. This beam-size measurement system plays an important role in the stable operation of the storage ring: the diagnosis of the stored beam and the control of the betatron coupling.

INTRODUCTION

The SAGA-LS is a synchrotron radiation facility operated by a local government, Saga prefecture in Japan [1]. This facility became operational in February, 2006. The SAGA-LS accelerator complex consists of a 255-MeV injector linac and a 1.4-GeV storage ring. In order to diagnose the stored beam, we have developed a beam-size measurement system. We adopted an SR interferometer [2] for the beam-size measurement. An interferogram is formed by synchrotron light (visible light) passing through a double-slit in the SR interferometer. The beam size can be obtained from the visibility (contrast) of the interferogram. In the case of direct focus systems (lens + CCD camera), the ambiguity of the beam size is large due to diffraction effects. The SR interferometer does not suffer from this problem.

DIAGNOSTIC BEAMLINE

We constructed a diagnostic beamline in order to extract visible light from the storage ring. The beamline is placed at BL20 in the SAGA-LS. Figure 1 shows the schematic layout of the BL20. This beamline is for light from the bending magnet (5° port). A water-cooled beryllium mirror (surface accuracy: $\lambda/4$) was installed in a vacuum chamber. The dimensions of the mirror are 33.6 mm (width) × 70 mm (height) × 45 mm (thickness). Since such a beryllium block is suitable for use as a mirror because of its rigidity and this type of mirror is used at other 1.5-GeV-class facilities [3, 4], we selected the beryllium mirror for use as an SR mirror. In the case of hard X-ray sources having a higher critical energy (e.g., KEK-PF [5]), thin transmission-type mirrors are often used to reduce the heat load. However, we did not adopt such a mirror, because most of the SR is absorbed in the mirror in the present case. We used an ICF152 window ($\lambda/10$) made of quartz to transmit the visible light. The effective diameter of the window was 100 mm, and the thickness was 10 mm. The air side of the window surface was coated with an anti-reflection film. In order to avoid contamination as a result of the strong light irradiation, the vacuum side of the surface was not coated [6]. The extracted visible light was directed to the darkroom using five mirrors ($\lambda/10$). The mirror diameter was 100 mm. The angle of rotation of the mirror (two-axis) can be controlled remotely using a stepping motor. The path of the visible light was covered with black boxes and pipes.

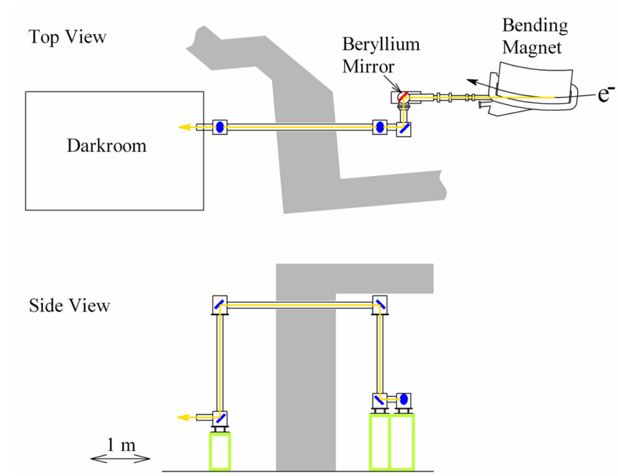

Figure 1: Layout (top and side views) of the diagnostic beamline BL20. The beryllium mirror (red) is in vacuum, and other mirrors (blue) are in air.

SR INTERFEROMETER

We set up an SR interferometer in the BL20 darkroom. Figures 2 and 3 show, respectively, a photograph and a schematic diagram of the interferometer. Visible light was sent to three measurement lines by dividing the light using half mirrors. One line is for bunch length measurement using a streak camera, and the other two lines are for horizontal and vertical interferometers. These measurement systems were placed on an optical table (1.5 m × 1.0 m). The interferometer consists of a double slit, an achromatic lens, a magnification lens, a Glan-Taylor prism, a band-pass filter, a neutral density (ND) filter, and a CCD camera. The slit width of the double-slit was 1 mm. The distance between the double slits was 4 mm for the horizontal interferometer, and 15 mm for the vertical interferometer. These slit distances were optimized by observing the contrasts of the interferograms. The focal length of the achromatic lens was f = 500 mm. The

#takabayashi@saga-ls.jp

magnification lens was used to enlarge the interferogram on the CCD camera. Indeed, we could not observe the visibility correctly without the magnification lens. The Glan-Taylor prism (extinction ratio: 5×10^{-5}) was used to select the polarization of light. We selected σ polarization, parallel to the bending plane. The bandwidth of the band-pass filter was ±5 nm for 500 nm (green light). We used a highly sensitive CCD camera (analog, black-and-white). The highly sensitive camera enables observation of the interferogram from a low-intensity beam.

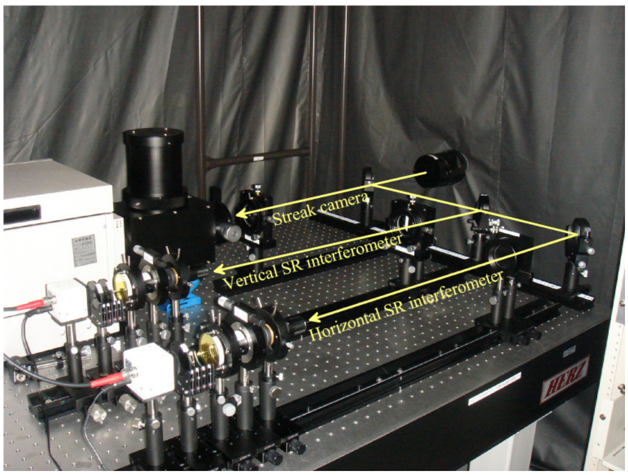

Figure 2: Photograph of the inside of the BL20 darkroom.

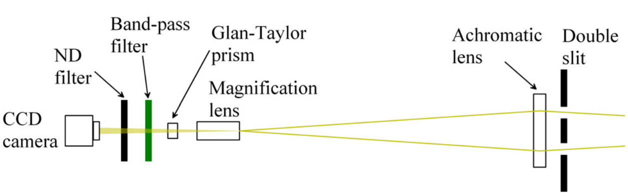

Figure 3: Schematic drawing of the SR interferometer.

DATA ACQUISITION SYSTEM

Figure 4 shows a schematic diagram of the data acquisition system. The interferogram observed using the CCD camera was acquired through a frame grabber board in a personal computer (PC). The measurement software was developed on LabVIEW. The front panel of the software is shown in Fig. 5. The one-dimensional profile is displayed together with the raw two-dimensional profile measured by the CCD camera. The one-dimensional profile was fitted to the following theoretical equation:

$$I(z) = I_0\left[\operatorname{sinc}\left(\frac{\pi w}{\lambda R}(z-z_1)\right)\right]^2 \times\left[1+\gamma\cos\left(\frac{2\pi D}{\lambda R}(z-z_2)\right)\right] + az + b. \quad (1)$$

Here, sinc(z) = sin(z)/z, z is x (horizontal) or y (vertical), w is the slit width, λ is the wavelength, R is the distance between the double-slit and the focal point, γ is the visibility, and D is the distance between the double slits. The last two terms in Eq. (1) represent the background. We used I_0, γ, a, b, c_1, c_2, c_3, and c_4 ($\pi w/\lambda R\cdot(z-z_1) = c_1 z + c_2$; $2\pi D/\lambda R\cdot(z-z_2) = c_3 z + c_4$) as fitting parameters. This fitting procedure was performed using the Levenberg-Marquardt method in LabVIEW. If the beam has a Gaussian distribution, the beam size can be obtained from the following equation:

$$\sigma = \frac{\lambda L}{\pi D}\sqrt{\frac{1}{2}\ln\left(\frac{1}{\gamma}\right)}, \quad (2)$$

where L is the distance between the light source and the double slit. In the present case, L is approximately 11 m.

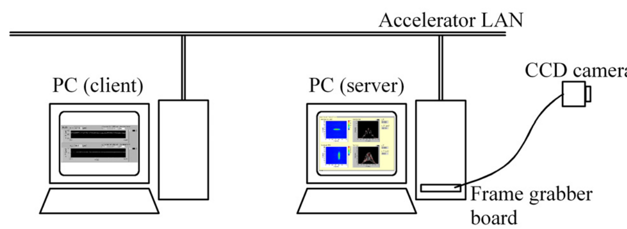

Figure 4: Schematic diagram of the client-server system.

We developed the client-server system based on the ActiveX CA, which is a protocol that operates in the Windows-PC environment [7]. The above-described software works as a server and publishes the obtained beam size. We also developed the client software with LabVIEW. Figure 6 shows the front panel of the client software in a console computer. The value of the beam size is displayed every 1 s. The trend graph of the beam size is also displayed.

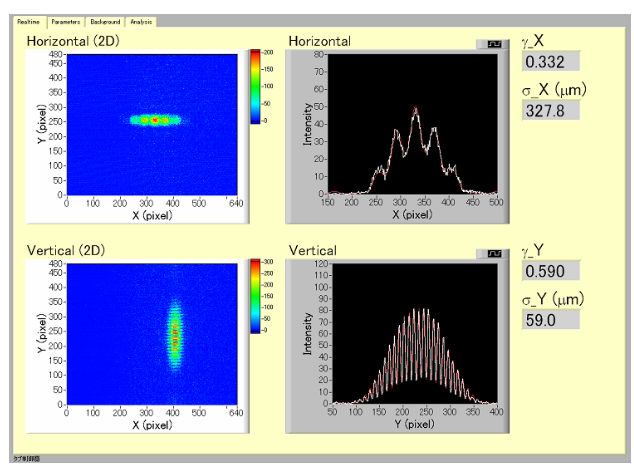

Figure 5: Front panel of the measurement software in the server PC.

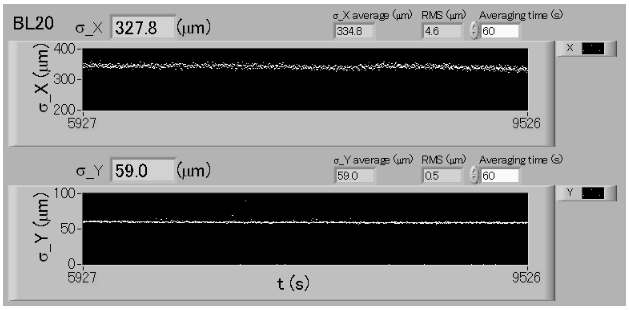

Figure 6: Front panel of the beam-size software in the console PC (client).

RESULTS AND DISCUSSION

Figure 7 shows the beam sizes measured in a typical user operation. Some data points deviated greatly from the average value in the vertical data. This is due to the fitting error. These errors must be reduced. The vertical beam size was in good agreement with the calculated value of 58 µm. In this calculation, we used a betatron coupling of 1.4%. This value was obtained from tune separation measurements around a difference-resonance condition [8]. However, the horizontal beam size did not agree with the calculated value of 203 µm. When we reduced the stored current to several mA, the horizontal beam size agreed with the calculation. Therefore, the observed discrepancy should be explained as follows. (i) The energy width of the electron beam increased with the beam current due to instabilities. The increase in the energy width leads to the increase in the horizontal beam size, because there is a finite dispersion in the bending magnet section. (ii) The deformation of the beryllium mirror is known to cause a shift in the beam size. This deformation is enhanced for a larger heat load (beam current). This effect can be corrected by a ray-trace method using a Hartmann-mask [2]. We recently installed a Hartmann-mask system to address this problem.

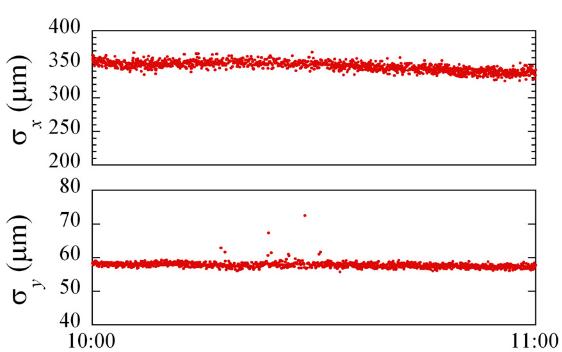

Figure 7: Typical horizontal and vertical beam sizes.

The proposed beam-size measurement system also plays an important role in the measurement of the betatron coupling. When we changed the gap of an undulator in the storage ring, the vertical beam size changed due to the skew quadrupole field of the undulator. We corrected the skew field by exciting a specially designed skew magnet so that the vertical beam size remains constant [9].

SUMMARY

We have developed a beam-size measurement system for the SAGA-LS storage ring. We adopted an SR interferometer as a method of beam-size measurement. We also developed a client-server system using the ActiveX CA protocol for data transmission. This beam-size measurement system is useful for monitoring the beam stability and controlling the betatron coupling.

ACKNOWLEDGMENT

The authors would like to thank Prof. Mitsuhashi (KEK) for providing advice on the diagnostic beamline BL20 and the SR interferometer.

REFERENCES

[1] T. Tomimasu *et al.*, "Commissioning of SAGA Light Source", PAC'05, Knoxville, May 2005, RPAE078, p. 4021 (2005).
[2] T. Mitsuhashi, "Twelve Years of SR Monitor Development at KEK", Beam Instrumentation Workshop, 2004.
[3] T.C. Tseng *et al.*, "The SRI Beam Size Monitor Developed at NSRRC", PAC'05, Knoxville, May 2005, RPAT059, p. 3465 (2005).
[4] Y. Shoji and K. Takeda, "Beryllium Mirror for Electron Beam Diagnostics Using Visible Synchrotron Radiation Light at NewSUBARU", Proceedings of the 5th Annual Meeting of Particle Accelerator Society of Japan, p. 740 (2008).
[5] T. Mitsuhashi and M. Kato, "A Construction of Optical Beam Profile Monitor for High Brilliance Configuration of the Photon Factory", EPAC'96, Sitges, June 1996, TUP053L, p. 1669 (1996).
[6] J.W. Flanagan *et al.*, "Amelioration of SR Extraction Window Transmission Loss via Elimination of Anti-reflective Coating", Proceedings of the 3rd Annual Meeting of Particle Accelerator Society of Japan, p. 681 (2006).
[7] H. Ohgaki *et al.*, "PC-LabVIEW Based Control System in SAGA-LS", PAC'05, Knoxville, May 2005, FPAT076, p. 3976 (2005).
[8] S. Koda *et al.*, "Measurement of Betatron Coupling in SAGA-LS Storage Ring", Proceedings of the 5th Annual Meeting of Particle Accelerator Society of Japan, p. 701 (2008).
[9] T. Kaneyasu *et al.*, "Characterization of the Effect of the Variably Polarized Undulator on Electron Beam at the SAGA-LS Storage Ring", Proceedings of the 6th Annual Meeting of Particle Accelerator Society of Japan, to be published.